Unusual magnetic behaviour of the disordered antiferromagnetic compound $NdAl_{0.8}Ga_{1.2}$ studied by neutron scattering

1990 J. Phys.: Condens. Matter 2 4737

(http://iopscience.iop.org/0953-8984/2/21/008)

J. Phys.: Condens. Matter 2 (1990) 4737–4746. Printed in the UK

Unusual magnetic behaviour of the disordered antiferromagnetic compound $NdAl_{0.8}Ga_{1.2}$ studied by neutron scattering

O Elsenhans†, A Furrer†, K N Clausen‡ and E Walker§

† Labor für Neutronenstreuung, ETH Zürich, c/o PSI, CH-5232 Villigen PSI, Switzerland

‡ Riso National Laboratory, DK-4000 Roskilde, Denmark

§ Département de Physique de la Matière Condensée, Université de Genève, CH-1205 Genève, Switzerland

Received 16 November 1989, in final form 12 February 1990

Abstract. Neutron diffraction, diffuse critical and inelastic neutron scattering experiments on a single crystal of the disordered antiferromagnetic compound $NdAl_{0.8}Ga_{1.2}$ are described. Below $T_N = 5.7$ K an incommensurate cycloidal spin structure of the Nd ions is observed. Both the Nd moments and the propagation vector are perpendicular to the c axis. The zero-field magnetisation exhibits a peculiar temperature dependence giving rise to an apparent critical exponent $\beta > 1$. This can most likely be attributed to the presence of competing single-ion interactions, due to the inherent disorder of the compound. The short-range ordered spin fluctuations are found to diverge at T_N. The crystalline electric field parameters are determined from inelastic neutron scattering experiments in the paramagnetic state. The energy spectra taken in the magnetically ordered state exhibit little dispersion and are thus analysed in the molecular field approximation.

1. Introduction

In recent years the study of disordered magnetic systems has attracted much interest. The disorder usually gives rise to random fields and competing interactions which may be elucidated in great detail by neutron scattering (Cowley *et al* 1984). Here we present a neutron scattering study of the disordered antiferromagnetic compound $NdAl_{0.8}Ga_{1.2}$ which may be considered as a random magnetic system with competing single-ion interactions.

A comprehensive experimental study of the crystalline and magnetic structures of the compounds $NdAl_pGa_{2-p}$ ($0 \leqslant p \leqslant 2$) was performed by Martin and Girgis (1983) and Martin *et al* (1983). $NdAl_pGa_{2-p}$ has cubic symmetry ($MgCu_2$ type) for $2 > p > 1.7$. For $1.7 > p > 1.4$ there is a two-phase region in which the cubic structure coexists with a hexagonal structure of the AlB_2 type. The latter is stabilised for $1.4 > p > 0$, but in the range $1.2 > p > 1.0$ a drastic change of the c/a ratio is observed with $c/a \simeq 0.85$ for $p > 1.2$ ('low' c/a) and $c/a \simeq 1$ for $p < 1.0$ ('intermediate' c/a). For $1.2 > p > 1.0$ the two hexagonal phases coexist. The magnetic structure was found to completely change with varying chemical structure types, ferromagnetic ordering is observed for the cubic phase, whereas antiferromagnetic ordering is realised for the hexagonal phases. For

0953-8984/90/214737 + 10 $03.50

$p > 1.2$ the spin direction is parallel to the c axis with modulation wave vector $\boldsymbol{k}_0 = (1/2, 0, 1/2)$, but perpendicular to the c axis with $\boldsymbol{k}_0 = (\zeta_0, 0, 0)$ for $p < 1.0$. All these findings indicate the presence of strong magneto-structural correlations in the $NdAl_pGa_{2-p}$ systems.

The origin of the magneto-structural correlations of $NdAl_pGa_{2-p}$ was examined in detail by Furrer and Martin (1986). They performed inelastic neutron scattering experiments and determined the crystalline electric field (CEF) interaction for $p = 1.75$, 1.25, 1, 0.5, 0. They demonstrated that the magnetic properties of $NdAl_pGa_{2-p}$ are indeed governed by distinct magneto-structural correlations. For a certain aluminium concentration p the CEF potential is essentially determined by geometrical coordination, so that the behaviour of the CEF parameters upon structural deformation can be reliably predicted. In particular, phase diagrams were calculated in order to study the transition from the modulated magnetic structure of NdAlGa to the antiferromagnetic structure realised for $NdAl_{1.25}Ga_{0.75}$. This phase transition cannot be investigated by varying the aluminium concentration p, since two crystallographically different phases coexist in the correponding 'crossover' region (Martin and Girgis 1983), however, it can be reached by application of uniaxial pressure which reduces the c/a ratio. The calculated phase diagram exhibits a Lifshitz point, i.e., a multicritical point separating a uniformly ordered phase, a modulated phase and a disordered phase. So far the only examples of systems passing through a Lifshitz point are MnP (Shapira 1982) and possibly $NiBr_2$ (Day *et al* 1984), and NdAlGa appears to be the first metallic system exhibiting a Lifshitz point. In fact, it was this particular feature which motivated us to perform the present study.

Unfortunately, the envisaged pressure experiments on single crystals of NdAlGa failed, since the crystals broke under uniaxial pressure below 1 kbar, so that we were unable to verify the predicted Lifshitz point. Nevertheless, we carried out elastic, diffuse critical and inelastic neutron scattering experiments on a single crystal of $NdAl_{0.8}Ga_{1.2}$ in order to study in detail the magnetic ordering, the spin fluctuations and the magnetic excitation spectrum, all of which gave evidence for an unusual critical behaviour of the system. In particular, the zero-field magnetisation was found to exhibit a peculiar initial temperature dependence below $T_N = 5.7$ K with an apparent exponent $\beta > 1$.

The organisation of this paper is as follows. Section 2 summarises the relevant experimental details. The results on the magnetic ordering, the critical scattering and the magnetic excitations are presented and analysed in section 3. Some final conclusions are discussed in section 4.

2. Experimental details

Single crystals of NdAlGa were grown using the standard Czochralski technique. The elements (5N Ga from Alusuisse, 5N Al and 3N Nd from Johnson–Matthey) were first melted together in a levitation crucible. The growth process was carried out in a RF heated tungsten crucible. To reduce evaporation, we applied one atmosphere of 4N7 Argon. A titanium filament was heated in the furnace during the process to remove as much oxygen as possible. The crystal was pulled at 15 mm h^{-1}, rotating the seed (obtained by the necking technique) at 12 turns min^{-1}.

The limit of the pure 'intermediate' c/a phase domain is at 50 at.% $NdGa_2$ as reported by Martin and Girgis (1983). However, starting with this composition, we were unable to obtain a single crystal, presumably because the presence of a small amount of the

'low' c/a phase. For this reason we increased the concentration of the melt to 55 at.% $NdGa_2$.

The shape of the crystals was approximately cylindrical with a diameter varying from 2 to 7 mm and a volume of typically 300 mm^3. Most of the crystals showed a relatively poor mosaicity up to 20 degrees. For the present neutron scattering experiments we used a crystal with a mosaicity of 5 degrees and a volume of about 250 mm^3. The composition of the crystal as determined at both ends by chemical analysis turned out to be $Nd_{1.00}Al_{0.78}Ga_{1.22}$, and the variation of the Al- and Ga-concentration was found to be less than 5 at.% along the cylindrical axis of the crystal.

Neutron diffraction and diffuse critical neutron scattering experiments were carried out at the reactor Saphir in Würenlingen with use of a double-axis diffractometer with a collimation of 60′ between the sample and the detector. A graphite monochromator provided a beam with a neutron wavelength of 0.234 nm.

One set of inelastic neutron scattering experiments were performed with use of the TAS7 triple-axis spectrometer installed at the neutron guide tube of the cold neutron source of the Riso DR-3 reactor. The incoming neutrons were scattered from a vertically bent graphite monochromator, and the energy of the horizontally bent graphite analyser was kept fixed at 5 meV, giving rise to an energy resolution ($\Delta E = 0$) of 0.15 meV. Another set of inelastic neutron scattering measurements were carried out on a triple-axis spectrometer at Würenlingen using a doubly bent graphite monochromator and a horizontally bent graphite analyser with fixed energy at 14.94 and 4.7 meV, giving rise to energy resolutions ($\Delta E = 0$) of 0.95 meV and 0.15 meV, respectively. All the triple-axis scans were carried out in the neutron energy-loss configuration.

In all experiments various Be and pyrolitic graphite filters were used to reduce higher order contaminations.

3. Results and Data Analysis

3.1. Magnetic Ordering

Figure 1 displays neutron diffraction patterns of single-crystalline $NdAl_{0.8}Ga_{1.2}$ performed along the [100] direction through the nuclear (100) reflection. Below $T_N = 5.7$ K there is clear evidence for the occurrence of magnetic satellites at (100) $\pm \boldsymbol{k}$ which rapidly grow with decreasing temperature, whereas the intensity of the nuclear Bragg peak remains constant. We have observed the magnetic satellites at various other nuclear ($h0l$) reflections. q-scans performed perpendicular to the [100] direction clearly indicated that the magnetic satellites occur along the [100] axis. The magnetic contributions are interpreted by an incommensurate antiferromagnetic ordering of the Nd sublattice corresponding to a cycloidal spin structure of the Nd magnetic moments with a magnetic wave vector $\boldsymbol{k} = (\frac{1}{8} - \delta, 0, 0)$, $\delta(T = 1.5\ \text{K}) = 2.67 \times 10^{-3}$. The magnetic moments of the Nd ions rotate in the basal plane and are oriented perpendicular to the c axis. This observation is in agreement with the corresponding work on polycrystalline samples (Martin *et al* 1983).

The quantitative evaluation of the observed neutron intensities suffered from the large mosaicity of the single crystal. This is reflected in the relatively large standard deviation of the resulting ordered magnetic moment of the Nd ions, which turned out to be $\mu_{Nd} = 1.5\ (5)\ \mu_B$ for a reliability factor $R_{wp} = 20\%$. The refinement of the single

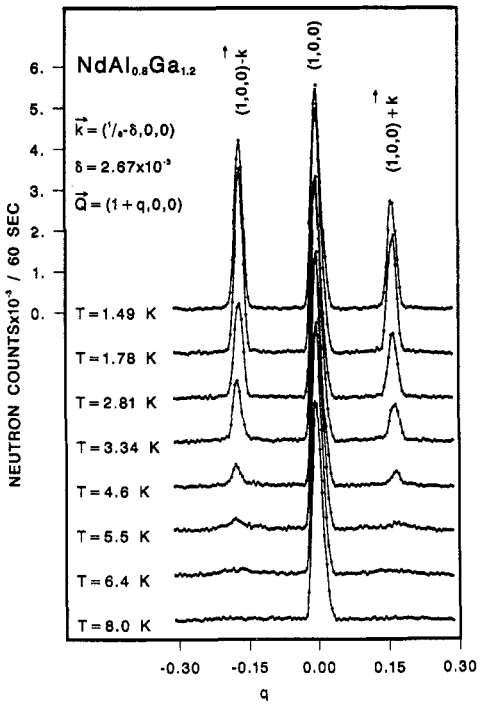

Figure 1. Temperature dependence of neutron diffraction scans observed for $NdAl_{0.8}Ga_{1.2}$.

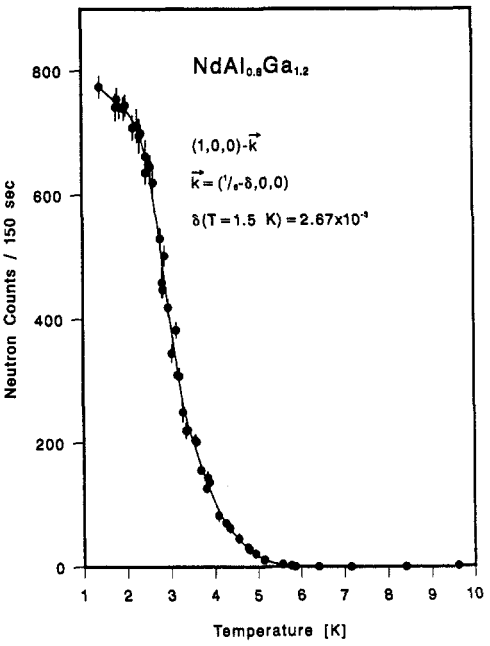

Figure 2. Temperature dependence of the integrated neutron scattering intensity of the antiferromagnetic Bragg peak (1 0 0)-***k*** observed for $NdAl_{0.8}Ga_{1.2}$. The diffuse critical neutron scattering contribution is subtracted from the data. The line is a guide to the eye.

crystal neutron scattering intensities was carried out with use of the computer program MINREF (Elsenhans 1989).

The temperature dependence of the integrated intensity of the magnetic satellite (100)-***k*** is shown in figure 2. The thermal variation is very unusual: The intensity exhibits a sudden drop above 2.5 K, but the final decrease towards T_N is rather slow. The absence of hysteresis effects clearly indicates a second-order phase transition. The temperature dependence of the observed magnetic propagation vector ***k*** is shown in figure 3. For temperatures above 2.5 K, where we observe the unusual behaviour of the peak intensity, the modulus of the wavevector ***k*** decreases with decreasing temperature, but still remains incommensurate with the nuclear cell symmetry.

3.2. Critical scattering

In order to study the unusual temperature dependence of the magnetic satellites in more detail diffuse critical neutron scattering experiments were performed. Figure 4 shows scans along [100] through the magnetic satellite (100)-***k*** for different temperatures in the critical temperature region. Above T_N we observe ordinary Lorentzian shaped diffuse intensity which increases with decreasing temperature. For $T \leq 5.7$ K, in addition to the diffuse intensity, a sharp (100)-***k*** Bragg peak is superimposed on the Lorentzian and this

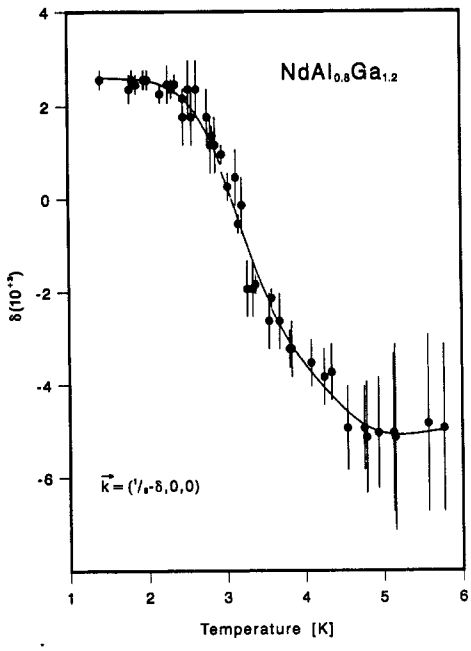

Figure 3. Temperature dependence of the magnetic wavevector $\boldsymbol{k} = (\frac{1}{8} - \delta, 0, 0)$ determined for $NdAl_{0.8}Ga_{1.2}$. The line is a guide to the eye.

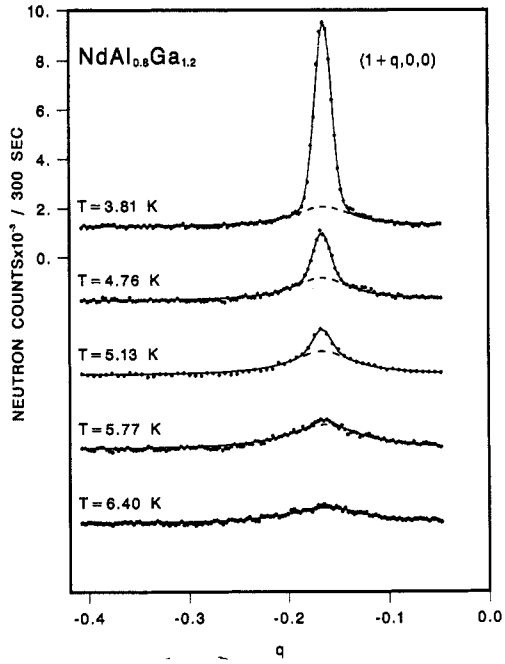

Figure 4. Neutron scattering scans through the antiferromagnetic peak (100)-$\boldsymbol{k}$ for different temperatures in the critical temperature range. The solid and dashed lines are Gaussian and Lorentzian fits to the neutron diffraction and diffuse critical scattering, respectively.

grows very rapidly with decreasing temperature. At all temperatures the half-width of the sharp peak corresponds to the instrumental resolution.

In figure 5 the temperature dependence of the scattering intensities for different deviations q from (100)-$\boldsymbol{k}$ are shown. For $q \geqslant 0.02$, where the Lorentzian of the diffuse scattering is not seriously contaminated by the strong Bragg peak, a maximum of the intensity is observed at the Néel temperature $T_N = 5.7$ K. An identical behaviour was found on both double- and triple-axis spectrometers, confirming the applicability of the quasistatic approximation to the observed diffuse neutron scattering intensity, which is proportional to the static part of the wavevector dependent susceptibility (Lovesey 1984).

The Lorentzian peak of the diffuse scattering samples the short-range ordered quasistatic spin fluctuations (Lovesey 1984). The inverse halfwidths of the Lorentzian peaks directly determine the mean correlation length ξ of the fluctuations which, however, could not be reliably determined from the experimental data because of the large mosaicity of the crystal.

3.3. Inelastic neutron scattering

Figure 6 shows typical energy spectra taken in the paramagnetic state at $T = 10$ K for several scattering vectors $\boldsymbol{Q}$. For the Ga rich compounds the overall CEF splitting is rather small (Furrer and Martin 1986). Consequently a large number of crystal-field transitions

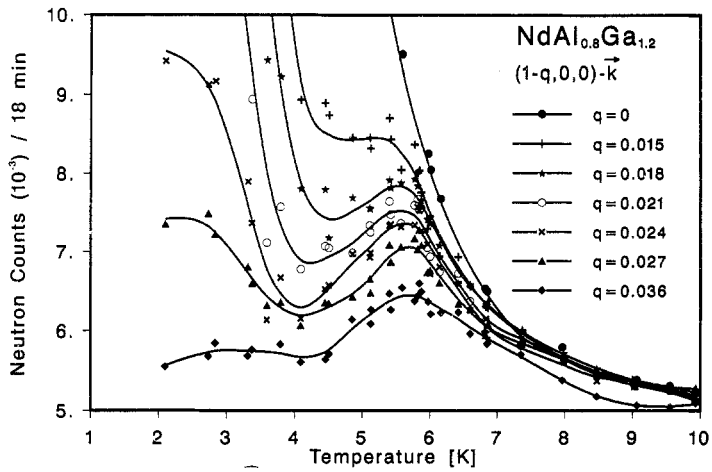

Figure 5. Temperature dependence of neutron scattering intensity for different deviations q from the antiferromagnetic satellite position (1, 0, 0)-$\boldsymbol{k}$. The lines are guides to the eye.

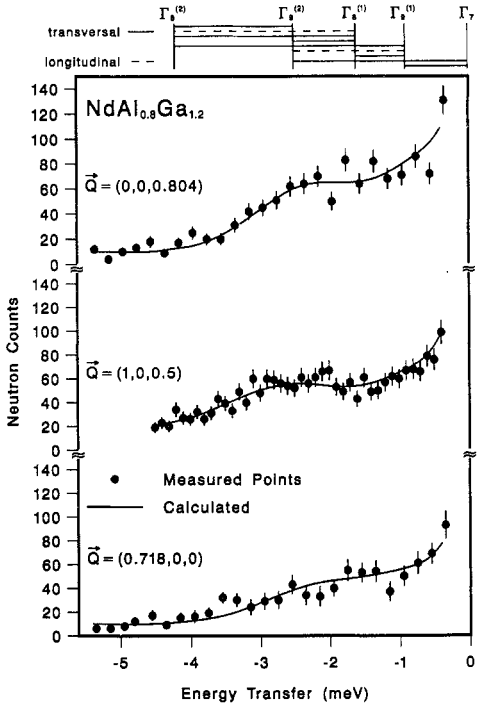

Figure 6. Energy spectra of neutrons scattered from $NdAl_{0.8}Ga_{1.2}$. $T = 10$ K, $E_A = 5$ meV. The lines are the result of a least-squares fit as explained in the text. The top of the figure shows the resulting energy level scheme.

contribute to the scattering at low energies, so that the observed energy spectra do not exhibit well resolved lines and a profile-type analysis has to be adopted. For $NdAl_{0.8}Ga_{1.2}$ the Nd^{3+} ions have the hexagonal site symmetry D_{6h}, thus the CEF Hamiltonian takes the form

$$\hat{H}_{\mathrm{CEF}} = B_2^0\hat{O}_2^0 + B_4^0\hat{O}_4^0 + B_6^0\hat{O}_6^0 + B_6^6\hat{O}_6^6, \tag{1}$$

where the B_n^m denote the CEF parameters and the $\hat{O}_n^m$ are operator equivalents (Stevens

1952). Equation (1) gives rise to a decomposition of the ground-state J-multiplet $^4I_{9/2}$ of the Nd^{3+} ions into five doublets, namely Γ_7, $2 \times \Gamma_8$, $2 \times \Gamma_9$. For a system of N non-interacting ions the differential neutron cross-section for the CEF transition $\Gamma_n \rightarrow \Gamma_m$ in the dipole approximation is given by (Trammell 1953)

$$\frac{d^2\sigma}{d\Omega\, d\omega} = \frac{N}{Z}\left(\frac{\gamma e^2}{m_e c^2}\right)^2 \frac{k_1}{k_0} \exp(-2W(\boldsymbol{Q}))F^2(\boldsymbol{Q}) \exp\left(\frac{-E_n}{k_B T}\right) \times \sum_{\alpha=x,y,z} [1 - (Q_\alpha/Q)^2] |\langle \Gamma_m | \hat{J}_\alpha | \Gamma_n \rangle|^2 \delta(E_n - E_m + \hbar\omega) \tag{2}$$

where Z is the partition function, k_0 and k_1 are the wavenumbers of the incoming and scattered neutrons, respectively, $\exp(-2W(\boldsymbol{Q}))$ is the Debye–Waller factor, $F(\boldsymbol{Q})$ the magnetic form factor, E_n the energy of the CEF state Γ_n, and $\hat{J}_\alpha$ the transverse ($\hat{J}_x$, $\hat{J}_y$) or longitudinal ($\hat{J}_z$) component of the total angular momentum operator. The remaining symbols have their usual meaning. The δ-function in (2) is usually replaced by a Gaussian because of line broadening due to relaxation effects, lattice distortions and instrumental resolution.

The polarisation factor $[1 - (Q_\alpha/Q)^2]$ in (2) permits discrimination between CEF transitions with different polarisation by measuring at different scattering vectors $\boldsymbol{Q}$. For $\boldsymbol{Q}$ parallel to the c axis the longitudinal transitions are completely suppressed, whereas for all the other directions of $\boldsymbol{Q}$ the observed spectra correspond to a weighted superposition of longitudinal and transverse transitions.

A least-squares fitting procedure was applied to the observed energy spectra on the basis of (2). For the initial values we used the CEF parameters derived from measurements on polycrystalline NdAlGa (Furrer and Martin 1986). Perfect convergence was achieved for the following CEF parameters:

$$B_2^0 = (0.9 \pm 0.1) \times 10^{-2}\ \text{meV}$$
$$B_4^0 = (-0.65 \pm 0.05) \times 10^{-3}\ \text{meV}$$
$$B_6^0 = (0.16 \pm 0.02) \times 10^{-4}\ \text{meV}$$
$$B_6^6 = (0.23 \pm 0.07) \times 10^{-3}\ \text{meV}.$$

The resulting CEF level scheme is shown on top of figure 6.

In addition to the measurements in the paramagnetic state we have also performed experiments below T_N. A series of energy spectra were taken at $T = 1.3$ K at various points in reciprocal space, and complete scans were performed along the [100] and [001] directions. The data analysis, however, was severely hampered by both the large linewidths of the excitations and the superposition of the magnetic Brillouin zones associated with the $\pm\boldsymbol{k}$ satellites. A representative energy spectrum is shown in figure 7 for $\boldsymbol{Q} = (0.5, 0, 1)$ where the $\pm\boldsymbol{k}$ satellites equally contribute to the scattering. There is a strong excitation at 0.6 meV with a shoulder at 1.3 meV. Since the excitations did not exhibit significant dispersion, we may analyse the data in the molecular field approximation. The system is then described by the Hamiltonian

$$\hat{H} = \hat{H}_{CEF} - \sum_\alpha \lambda_\alpha \langle \hat{J}_\alpha \rangle \hat{J}_\alpha \tag{3}$$

where λ_α are the molecular field parameters. The moleular field part of (3) further splits the CEF doublets into molecular field singlet states. In the calculations we have taken $\lambda_x = \lambda_y = 0.058$ meV and $\lambda_z = 0.260$ meV which is consistent with $T_N = 5.7$ K and $\boldsymbol{\mu} \perp \boldsymbol{c}$,

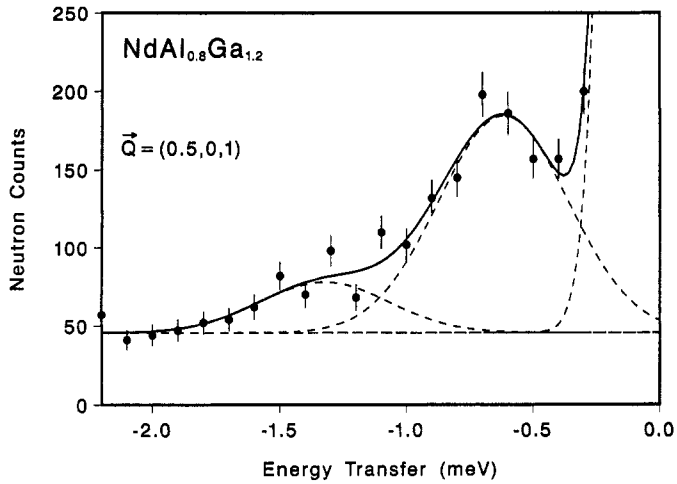

Figure 7. Energy spectrum of neutrons scattered from $NdAl_{0.8}Ga_{1.2}$. $T = 1.3$ K, $E_A = 5$ meV. The lines are the results of a Gaussian least-squares fit.

i.e., $\langle \hat{J}_z \rangle = 0$. Equation (3) then gives rise to low-lying transverse excitations at 0.8 meV (corresponding to the splitting of the ground-state doublet Γ_7) and 1.4 meV. Both the energies and intensities of these excitations are in reasonable agreement with the observations and thereby support the derived CEF level scheme.

4. Discussion

In figure 8 we compare the structural magnetic data for single crystalline $NdAl_{0.8}Ga_{1.2}$ as determined in the present work with the values obtained for polycrystalline $NdAl_pGa_{2-p}$ (Martin *et al* 1983). For $NdAl_{0.8}Ga_{1.2}$ the modulation wavevector $\boldsymbol{k}$ as well as the magnetic moment μ can reasonably be interpolated from the polycrystalline data, whereas the Néel temperature exceeds the interpolated value by a factor 2. This discrepancy readily demonstrates the difficulty in accurately determining T_N from powder diffraction, whenever the temperature dependence of the magnetic Bragg scattering exhibits an unusual behaviour. In particular, critical scattering can only be separated from Bragg scattering in single crystal experiments. From the present experiments we undoubtedly arrived at a reliable value of $T_N = 5.7$ K, since at that temperature we observe both the onset of long-range magnetic ordering (see figure 4) and the divergence of the magnetic susceptibility (see figure 5).

CEF effects significantly influence the thermodynamic magnetic properties, which may therefore serve as an experimental check for the CEF parameters. We have calculated the zero-field magnetisation of $NdAl_{0.8}Ga_{1.2}$ in the molecular field approximation and found $\mu = 2.4\mu_B$ at saturation which is slightly outside the error bar of the observed value (see figure 8). The difference between the observed and calculated value may be due to conduction-electron polarisation and J-mixing effects (Furrer and Tellenbach 1975). With the second-order CEF parameters $B_2^0 > 0$ the easy axis of the magnetisation is forced to lie in the basal plane as experimentally verified in the present work.

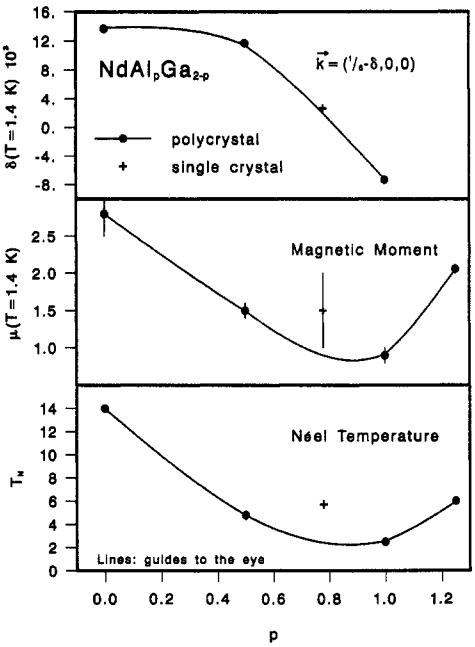

Figure 8. Néel temperature, zero-field magnetisation and modulation wavevector of $NdAl_pGa_{2-p}$. The dots correspond to the polycrystalline data determined by Martin *et al* (1983), and the crosses are the single crystal results obtained in the present work.

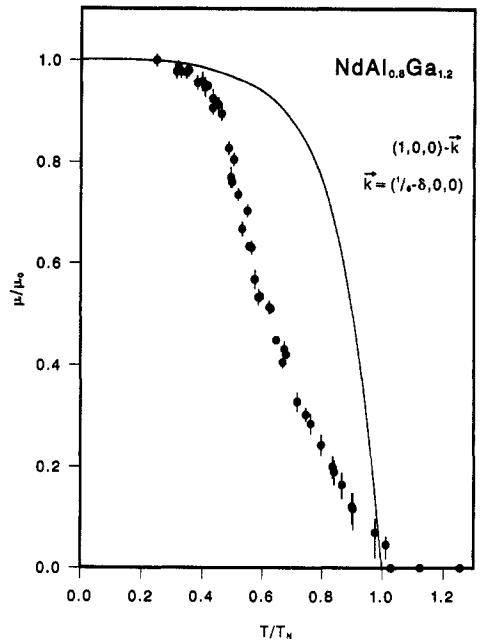

Figure 9. Zero-field magnetisation of $NdAl_{0.8}Ga_{1.2}$ versus temperature in reduced units. The circles represent the experimental data obtained in the present work. The line corresponds to a mean-field calculation as explained in the text.

Figure 9 shows the comparison between the observed and calculated zero-field magnetisation in reduced units. Although a mean-field calculation is known to be a poor approximation close to T_N, the discrepancy between theory and experiment is unexpectedly large. A similar unusual critical temperature dependence of the order parameter below T_N with an apparent exponent $\beta > 1$ has recently been observed in CeAs (Hälg *et al* 1987) and YbAs (Dönni *et al* 1989). Obviously the short-range ordered spin fluctuations strongly suppress the development of the long-range ordered magnetisation. For CeAs and YbAs the extraordinarily large spin fluctuations have tentatively been attributed to the almost isotropic nature of the CEF ground state, so that as a result the magnetic moments are not fixed in a certain direction, but can turn around in a way compatible with the corresponding magnetic ordering. This explanation certainly does not hold for $NdAl_{0.8}Ga_{1.2}$, since the CEF interaction gives rise to a highly anisotropic ground state with $g_\perp = 3.6$ and $g_\parallel = 0.7$. We rather feel that the unusual critical behaviour is due to random fields or random anisotropy induced by the inherent disorder of the sample. In particular, there is a strong competition of single-ion interactions at the Nd^{3+} sites which on the average have a Ga-rich surrounding, favouring $\boldsymbol{\mu} \perp \boldsymbol{c}$, but statistical considerations show that there are also Nd^{3+} sites with an Al-rich surrounding favouring $\boldsymbol{\mu} \parallel \boldsymbol{c}$. This competition presumably manifests itself also in the large temperature dependence of the ordering wavevector $\boldsymbol{k}$ above 2.5 K, see figure 3. An alternative explanation would be to postulate a series of successive phase transitions above 2.5 K which have not been detected because of the large mosaic spread of the single crystal. Indeed the

zero-field magnetisation exhibits an apparent discontinuity at around 3 K where the ordering wavevector $\boldsymbol{k}$ changes rapidly, see figures 3 and 9, thus a 'lock-in' of the magnetic structure at the commensurate $\boldsymbol{k} = (\frac{1}{6}, 0, 0)$ cannot be ruled out. At present we have no model that is able to describe these effects on a quantitative level.

Acknowledgment

Financial support by the Swiss National Science Foundation is gratefully acknowledged.

References

Cowley R A, Birgeneau R J, Shirane G and Yoshizawa H 1984 *Multi-critical Phenomena* ed R Pynn and A Skjeltorp (New York: Plenum) p 333
Day P, Moore M W, Wood T E, Paul D Mck, Ziebeck K R, Regnault L P and Rossat-Mignod J 1984 *Solid State Commun.* **51** 627
Dönni A, Fischer P, Furrer A and Hulliger F 1989 *Solid State Commun.* **71** 365
Elsenhans O 1990 *J. Appl. Crystallogr.* **23** 73
Furrer A and Martin O E 1986 *J. Phys. C: Solid State Phys.* **19** 3863
Furrer A and Tellenbach U 1975 *Helv. Phys. Acta* **48** 451
Hälg B, Furrer A and Kjems J K 1987 *Phys. Rev. Lett.* **59** 1034
Lovesey S 1984 *Theory of Neutron Scattering from Condensed Matter* vol 2 (Oxford: Clarendon) p 310
Martin O E and Girgis K 1983 *J. Magn. Magn. Mater.* **37** 228
Martin O E, Girgis K and Fischer P 1983 *J. Magn. Magn. Mater.* **37** 231
Shapira Y 1982 *J. Appl. Phys.* **53** 1914
Stevens K W H 1952 *Proc. Phys. Soc.* A **65** 209
Trammell G T 1953 *Phys. Rev.* **92** 1387